Proteomic analysis of inhibitor of apoptosis protein-like protein-2 on breast cancer cell proliferation

SIQI XIANG[1,2*], LIN ZHU[1*], ZHILIANG ZHANG[1*], SIYUAN WANG[1], RUXIA CUI[1] and MINGJUN XIANG[1]

[1]Department of Biochemistry and Immunology, Medical Research Center, Institute of Medicine, Jishou University, Jishou, Hunan 416000; [2]Department of Bioengineering, Biological Science and Engineering School, North Minzu University, Yinchuan, Ningxia 750021, P.R. China

Received October 6, 2021; Accepted December 10, 2021

DOI: 10.3892/mmr.2022.12605

Abstract. Although inhibitor of apoptosis protein-like protein-2 (ILP-2) is considered to be a novel enhancer of breast cancer proliferation, its underlying mechanism of action remains unknown. Therefore, the present study aimed to investigate the expression profile of ILP-2-related proteins in MCF-7 cells to reveal their effect on promoting breast cancer cell proliferation. The isobaric tags for relative and absolute quantification (iTRAQ) method was used to analyse the expression profile of ILP-2-related proteins in MCF-7 breast cancer cells transfected with small interfering (si)RNA against ILP-2 (siRNA-5 group) and the negative control (NC) siRNA. The analysis of the iTRAQ data was carried out using western blotting and reverse transcription-quantitative PCR. A total of 4,065 proteins were identified in MCF-7 cells, including 241 differentially expressed proteins (DEPs; fold change ≥1.20 or ≤0.83; P<0.05). Among them, 156 proteins were upregulated and 85 were downregulated in the siRNA-5 group compared with in the NC group. The aforementioned DEPs were mainly enriched in 'ECM-receptor interaction'. In addition, the top 10 biological processes related to these proteins were associated with signal transduction, cell proliferation and immune system processes. Furthermore, ILP-2 silencing upregulated N(4)-(β-N-acetylglucosaminyl)-L-aspar aginase, metallothionein-1E and tryptophan 2,3-dioxygenase, whereas ILP-2 overexpression exerted the opposite effect. The results of the present study suggested that ILP-2 could promote breast cancer growth via regulating cell proliferation, signal transduction, immune system processes and other cellular physiological activities.

Correspondence to: Professor Mingjun Xiang, Department of Biochemistry and Immunology, Medical Research Center, Institute of Medicine, Jishou University, 120 Renmin South Road, Jishou, Hunan 416000, P.R. China
E-mail: xmj688@163.com

*Contributed equally

Key words: breast cancer, inhibitor of apoptosis protein-like protein-2, isobaric tags for relative and absolute quantification, proteome

Introduction

Breast cancer is a common malignancy in women (1), with increasing incidence and mortality rates worldwide (2). In 2017, 252,710 new breast cancer cases were recorded in the United States (1). Although breast cancer therapies have improved, more breast cancer cases have been reported in recent years compared with 2008, possibly due to specific key risk factors, such as alcohol consumption, obesity and ageing (3). Therefore, novel treatment approaches and diagnostic tools for the early diagnosis of breast cancer are urgently required.

With the recent discovery of drugs targeting specific molecules in breast cancer, such as human epidermal growth factor receptor 2, epidermal growth factor receptor and the mammalian target of rapamycin signalling pathway, targeted therapy has been attracting increasing interest (4-6). It has been reported that inhibitor of apoptosis protein-like protein-2 (ILP-2) is upregulated in breast cancer cells and tissues, and promotes breast cancer growth (7). Protein expression levels of ILP-2 in breast cancer cell lines, such as MX-1 and MCF-7, have been found to be significantly increased when compared with those in the breast epithelial cell line MCF-10A, and small interfering (si)RNA-5 has demonstrated higher knockdown (KD) efficiency on ILP-2 than siRNA-3. A previous study from our laboratory suggested that ILP-2 could be considered a serological biomarker and a novel growth factor in breast cancer (8). However, the mechanism underlying the effect of ILP-2 on promoting breast cancer growth remains unknown.

Isobaric tag for relative and absolute quantitation (iTRAQ) is an accurate and reliable proteomic method used for quantitative analysis (9). This method is applied in proteomic analysis via combining liquid chromatography and tandem mass spectrometry (LC-MS/MS). These tags can be covalently linked to amino acids, including N-terminal amino acids and lysine side chain amino acids, through stable isotopically labelled molecules (10-12).

The present study aimed to investigate the expression profile of ILP-2-related proteins in MCF-7 cells to reveal the mechanism underlying the effect of ILP-2 on accelerating

breast cancer cell proliferation and to ascertain whether ILP-2 could act as a novel target for the targeted therapy of breast cancer.

Materials and methods

Cell culture and collection. MCF-7 and MX-1 cells lines were obtained from the American Type Culture Collection. Cell lines were cultured in RPMI-1640 medium (Gibco; Thermo Fisher Scientific, Inc.) supplemented with 10% foetal bovine serum (FBS; Gibco; Thermo Fisher Scientific, Inc.) and 1% Penicillin-Streptomycin mixture (Beijing Solarbio Science & Technology Co., Ltd.) in 5% CO_2 at 37˚C.

RNA interference. MCF-7 and MX-1 cell lines were divided into the siRNA-5 group (KD group), which targeted ILP-2, and the negative control (NC) group. According to the manufacturer's instructions, Lipofectamine® 2000 (Invitrogen; Thermo Fisher Scientific, Inc.) and siRNA [siRNA-5 (sense, 5'-CUAUAC GAAUGGGAUUUGATT-3' and antisense, 5'-UCAAAUCCC AUUCGUAUAGTT-3') and NC siRNA (sense, 5'-UUCUCC GAACGUGUCACGUTT-3' and antisense, 5'-ACGUGACAC GUUCGGAGAATT-3') (both from Shanghai GenePharma Co., Ltd.)] were individually mixed at 1:1 (volume ratio) and stored for 20 min at room temperature. Two groups of mixed siRNA (siRNA-5 and NC) and Lipofectamine 2000 were added to MCF-7 and MX-1 cells at a cell density of 50%, and cultivated in 5% CO_2 for 24 h at 37˚C. The siRNA had a final concentration of 100 nM (13,14). Total proteins and RNA were separately extracted, and then proteins and RNA were analysed via western blotting and reverse transcription-quantitative (RT-q)PCR analysis, respectively.

Overexpression plasmid vector construction. Plasmid vector GV219, restriction endonuclease *Xho*I/*Kpn*I, primers and *Escherichia coli* strains were obtained from Shanghai GeneChem Co., Ltd. The primers were designed based on the sequence of the coding region of the *BIRC-8* (*ILP-2*) gene in the National Center for Biotechnology Information. ID no. *BIRC8*(69070-1)-p1, 5'ACGGGCCCTCTAGACTCG AGACTCCACCGCGTGGTTTC-3' and *BIRC8* (69070-1)-p2, 5'-TTAAACTTAAGCTTGGTACCTTGAGTCACATCACAC ATTTAATC-3'. The target gene fragments were prepared and the digestion sites were constructed according to the vector requirements. The linearised vector and the target gene amplification products were used to formulate the reaction system, and the recombination reaction was carried out to achieve *in vitro* cyclisation of the linearised vector and the target gene fragment. The recombinant product was directly transformed and single clones from the plates were chosen for PCR identification, sequencing of positive clones and analysis of the results. The correct clone broth was expanded and extracted to obtain a high purity plasmid for subsequent experiments.

Plasmid extraction. The correctly sequenced bacteriophage was transferred to 10 ml lysogeny broth liquid medium (both from Shanghai GeneChem Co., Ltd.) containing the corresponding antibiotics (50 mg/l ampicillin), incubated overnight at 37˚C, and the plasmid was extracted using the Plasmid Small Extraction Medium Kit (Shanghai GeneChem Co., Ltd.). The overnight culture was collected in a labelled 5-ml centrifuge tube at 12,000 x g and centrifuged for 2 min at 4˚C to collect the bacterium. The supernatant was discarded, 250 μl cell resuspension solution was added and then shaken to keep the bacterium in suspension. Subsequently, 250 μl RIPA lysis buffer and 10 μl proteinase K was added, mixed gently by inverting up and down 5-6 times, and then left for 1-2 min to clarify the lysis. Neutralising Solution (350 μl) was added, mixed upside down to completely remove the protein and left for 5 min in an ice bath. Centrifugation was performed at 10,000 x g for 10 min at 4˚C, the protein was then discarded and the supernatant was collected in a clean, sterile 1.5 ml Eppendorf (EP) Tube®. Centrifugation was performed at 12,000 x g for 5 min at 4˚C and a labelled recovery column was prepared. The lower waste layer was discarded. Subsequently, 600 μl pre-programmed rinse solution was added, centrifuged at 12,000 x g for 1 min at 4˚C and the lower waste layer was discarded, this was repeated at 12,000 x g for 2 min at 4˚C to further remove the residual rinse solution. The column was transferred to a new 1.5-ml EP tube on the ultra-clean table and left to stand for 10-20 min to dry. Nuclease-Free Water (95 μl) was added to the recovery column, left for 2 min, centrifuged at 12,000 x g for 2 min at 4˚C, and the samples were collected for numbering, electrophoresis, determination of concentration and quality control.

According to the manufacturer's instructions, Lipofectamine 2000 and plasmid vector GV219 [GV219-ILP-2 and GV219 empty vector (NC)] were individually mixed at 1:1 (volume ratio) and stored for 20 min at room temperature. Mixed Lipofectamine 2000 and plasmid vector GV219 were added to MCF-7 and MX-1 cells (cell density of ~50%) and cultivated in 5% CO_2 for 24 h at 37˚C, wherein the plasmid vector GV219 (GV219-ILP-2 and NC) had a final concentration of 100 nM. Overexpression effects on ILP-2 expression were analysed by western blotting.

Mixed Lipofectamine 2000 and plasmid vector GV219 (GV219-ILP-2 and NC) were added to the MCF-7 and MX-1 cells in the logarithmic growth phase and cultivated in 5% CO_2 for 24 h at 37˚C. Total proteins were separately extracted from MCF-7 and MX-1 cells with RIPA buffer (Beyotime Institute of Biotechnology). MCF-7 and MX-1 cells were washed with 0.01 M PBS to remove the medium. Afterwards, a lysis buffer (7 M urea and 4% SDS) containing 1 mM phenyl-methane-sulfonyl fluoride was added to each group of cells ($1x10^7$ cells). The cells were lysed on ice for 30 min and then 12,000 x g for 5 min at 4˚C to extract the supernatant of the mixed solution for analysis, following which proteins were analysed via western blotting.

ITRAQ assays

SDS-PAGE and protein digestion. Total proteins of the aforementioned mixed solution from the two groups of cells (siRNA-5 and NC) were extracted from MCF-7 cells with RIPA buffer (Applygen Technologies, Inc.). Protein concentrations of isolated proteins in the aforementioned two groups were determined by a BCA protein assay kit (Applygen Technologies, Inc.). Protein concentrations of samples were adjusted to a constant level using the dilution. Total protein (20 μg/lane) was separated via SDS-PAGE on 10% gels. Proteins in the gels were cut into gel slices, and the gel bands were digested by an in-gel trypsin.

Table I. Liquid chromatography gradient of first dimensional separation of peptides.

Time, min	B, %
0	2
5	5
40	25
45	80
50	80
51	2
60	stop

Table II. Gradient elution of liquid chromatography and tandem mass spectrometry.

Time, min	B, %
0	2
70	40
70	90
75	90
75	2
90	2

Reductive alkylation and protease digestion. Dithiothreitol (20 mM final concentration) was added to extracted protein samples by SDS-PAGE (100 μg/μl), and the samples were incubated at 37˚C for 60 min. Iodoacetamide (40 mM final concentration) was added and the samples incubated in the dark at room temperature for 40 min. Pre-cooled acetone (volume ratio of 5:1) was added to the samples, and the mixture was placed at -20˚C for 2 h. The sediment was collected by centrifugation at 10,000 x g for 20 min at 4˚C and re-dissolved in 100 mM tetraethyl ammonium bromide buffer. Trypsin (1 mg trypsin/50 mg protein) was added to the protein samples, and settled at 37˚C overnight.

Isotope labelling. Protease-digested proteins were labelled with 113, 117, 114 and 118 isotopes. The NC group was labelled with 113 and 117 isotopes, whereas the siRNA-5 group was labelled with 114 and 118 isotopes. There were two biological replicates and three technical replicates. Peptides (100 μg) were labelled with an iTRAQ reagent tube (Applygen Technologies, Inc.) (15,16).

First dimensional separation of peptides. Separation of peptides was performed by ultra-high pressure liquid chromatography (UPLC) (Waters Corporation) with a 2.1x150 mm X Bridge BEH300 column (Waters Corporation). The moving phase was a mixture of water (pH adjusted to 10.0 with ammonia and formic acid) and acetonitrile, which was isocratically transmitted using a pump at a flow rate of 0.4 ml/min. The wavelength of the ultraviolet absorbance detector was 214/280 nm. The percentages used for gradient elution are listed in Table I. A total of 10 fractions were collected according to different retention times. Rotation vacuum concentrators (Christ RVC 2-25; Martin Christ Gefriertrocknungsanlagen GmbH) were used for concentration, and dissolved in buffer solution (pH adjusted to 10.0 with ammonia and formic acid) for further analysis.

LC-MS/MS. Labelled peptides were analysed using a NanoAcquity UPLC system (Waters Corporation) combined with a quadrupole-Orbitrap mass spectrometer (Q-Exactive; Thermo Fisher Scientific, Inc.), incorporating a C18 column (75 μm x 25 cm; Thermo Fisher Scientific, Inc.). The mobile phase was a mixture of water, with 2% acetonitrile and 0.1% formic acid isocratically delivered using a pump at a flow rate of 300 nl/min. The schemes used for gradient elution are shown in Table II. Full-scan mass spectrometry (350-1,300 m/z) was acquired with a first mass resolution of 70 K, and second resolution of 17.5 K (Chromeleon 7.3 CDS software; cat. no. CHROMELEON7; Thermo Fisher Scientific, Inc.). Fragmentation was used for high-energy collision dissociation. The micro scan was recorded using dynamic exclusion of 18 sec.

iTRAQ data analysis. The MS/MS data of iTRAQ were analysed using Proteome Discoverer Software version 2.1 (Thermo Fisher Scientific, Inc.) and searched in Unipr ot-proteomes-homo-sapiens-70611.fasta. The database had 70,611 entries and the date of download was July 15, 2016 [project ID. IPX0001520000; https://www.iprox.cn/page/PSV023.html;?url=1640500832317IEB0 (password, deZn)]. Result-filtered parameters were used to control peptide level false discovery rates ≤1%. Protein quantification was performed by only using unique peptides, and normalisation of protein medians was applied to rectify experimental deviation, which was accomplished by using retrieval software. The ratios of the samples were weighted, and normalised by contrasting the NC group (sample tagged as 113 and 117) to the denominator for protein quantitation. Regarding the quantitative changes, a ≥1.2 or ≤0.83 fold-change (FC) takeout and $P<0.05$ (t-test) were set for differentially expressed proteins (DEPs).

Gene Ontology (GO; http://www.geneontology.org/) and Kyoto Encyclopedia of Genes and Genomes (KEGG; http://www.genome.jp/kegg/) pathway analyses were applied to annotate and classify all authenticated proteins. The Database for Annotation, Visualization and Integrated Discovery (DAVID) version 6.8 Functional Annotation Tool (https://david.ncifcrf.gov/) was applied to process the DEPs for the enrichment analysis. Fisher's exact test was used to filter results. ClueGO of Cytoscape software (http://www.cytoscape.org/) was performed to assess GO biological networks. Search Tool for the Retrieval of Interacting Genes (STRING) version 10.0 (http://www.string-db.org/) was applied to analyse protein-protein interactions, and a high coefficient value of 0.7 was used as a cut-off. The expression patterns of DEPs (FC ≥1.2 or ≤0.83 and $P<0.05$) were identified by Cluster analysis using hcluster (https://pypi.python.org/pypi/hcluster/0.2.0) (9,17).

Western blot analysis. Cells in the siRNA-5 and NC groups ($5x10^6$ cells/group) were separately collected and western blot analysis was carried out. Total proteins were extracted from MCF-7 and MX-1 cells with RIPA buffer [150 mM

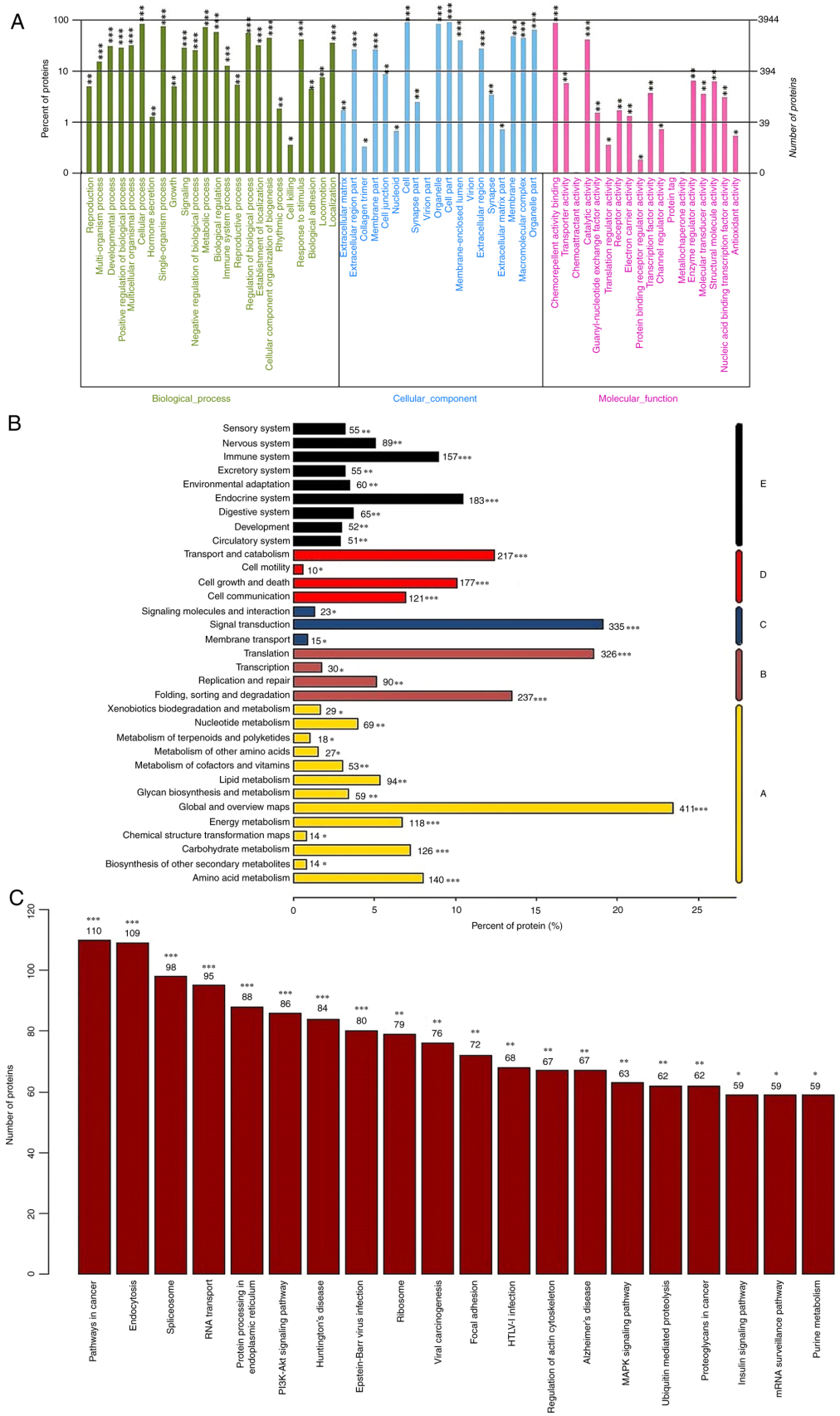

Figure 1. Functional classification of all annotated proteins associated with inhibitor of apoptosis protein-like protein-2 in MCF-7 cells. (A) Proteins classified into three main categories by Gene Ontology analysis, including biological process, cellular component and molecular function. The left y-axis indicates the percentage of a specific category of proteins in that category. The right y-axis indicates the number of proteins in the category. (B) Proteins were classified into five main categories by KEGG analysis, including 'metabolism', 'genetic information processing', 'environmental information processing', 'cellular processes' and 'organismal systems', indicated by A, B, C, D and E on the y-axis, respectively. The x-axis indicates the percentage of proteins within that specific category. (C) The number of proteins in the top 20 pathways determined by KEGG analysis. The y-axis indicates the number of proteins in the category. *P<0.05, **P<0.01, ***P<0.001 vs. the NC group. KEGG, Kyoto Encyclopedia of Genes and Genomes; NC, negative control.

NaCl, 20 mM Tris, 0.1% SDS (pH 7.5), 1% deoxycholate and 1% Triton X-100] supplemented with protease inhibitors. The protein concentration was determined using a BCA Protein Assay kit. Subsequently, total proteins (30 μg/per lane) were separated by SDS-PAGE on 10% gels at 70 V for 20 min and then at 100 V for 100 min. The proteins were then transferred onto PVDF membranes (Merck KGaA) at 350 mA for 105 min. After blocking with 5% skimmed milk powder in TBS with 0.05% Tween-20 (TBST) for 2 h at 37˚C, the membranes were incubated with primary antibodies against metallothionein 1E (MT1E; mouse IgG; 1:500; cat. no. MAD794Hu21; Cloud-Clone Corp.), ILP-2 (rabbit IgG; 1:1,000; cat. no. ab9664), tryptophan 2,3-dioxygenase (TDO2; rabbit IgG; 1:500; cat. no. ab84926), N(4)-(β-N-acetylglucosaminyl)-L-asparaginase (AGA; rabbit IgG; 1:500; cat. no. ab231021; all from Abcam), Tubulin (rabbit IgG; 1:1,000; cat. no. ab6046; Abcam) and GAPDH (mouse IgG; 1:2,500; cat. no. 60004-1-Ig; both from ProteinTech Group, Inc.) overnight at 4˚C. The next day, the membranes were washed with TBST and incubated with HRP-conjugated goat anti-rabbit IgG (1:5,000; cat. no. ab6728; Abcam) and HRP-conjugated AffiniPure goat anti-rabbit IgG (H+L) (1:5,000; cat. no. ZB-2301; OriGene Technologies, Inc.) for 1 h at room temperature. An ECL detection system (SuperECL-Plus; Applygen Technologies, Inc.) was utilized to visualise the immunoreactive proteins. The bands were semi-quantified with ImageJ v1.8.0.112 software (National Institutes of Health). Tubulin and GAPDH served as internal controls. Experiments were repeated at least three times.

RT-qPCR analysis. To separately extract the total RNA of the siRNA-5 and NC groups cells, the cell samples were washed twice with 1 ml PBS in a cell culture dish, 1 ml TRIzol® reagent (Invitrogen; Thermo Fisher Scientific, Inc.) was added and evenly pipetted for transfer into a 1.5 ml RNase-free EP tube to fully lyse the cells. This was left to stand at room temperature for 10 min, after which 200 μl chloroform was added, shaken vigorously for 15 sec and left to stand at room temperature for 10 min. Subsequently, this mixture was centrifuged at 4˚C at 12,000 x g for 15 min, the upper colourless liquid phase was collected in a new 1.5 ml RNase-free EP tube, 500 μl isopropanol was added, and then shaken and mixed well. After 10 min at room temperature, the mixture was centrifuged at 4˚C at 12,000 x g for 10 min and the supernatant was discarded; 1 ml 75% alcohol was added, gently shaken to wash the precipitate, centrifuged at 4˚C for 5 min at 12,000 x g and the supernatant was discarded, which was repeated twice. Subsequently, this was dried at room temperature for 15 min and 50 μl diethyl pyrocarbonate water was added to dissolve the RNA. The OD 260/280 of RNA was measured on the nucleic acid protein detector to detect the purity of total RNA, and the RNA sample was run via 1% agarose gel electrophoresis to detect RNA integrity. RT of RNA was performed according to the manufacturer's instructions of the qPCR RT Kit (Thermo Fisher Scientific, Inc.). The concentration of total RNA of the aforementioned two groups of cells was adjusted to 100 ng/μl. The components were added to a 0.2-ml RNase-free EP tube in the following order to prepare the RT reaction solution: 2 μl 5X RT Buffer, 0.5 μl RT Enzyme Mix, 0.5 μl Primer Mix, 1 μg RNA and the reaction solution was made to 10 μl by adding RNA-free water. For RT, the aforementioned mixture was loaded onto a PCR machine, and RT was performed at 37˚C for 15 min and at 98˚C for 5 min, and the cDNA was stored at 4˚C for immediate use or at -20˚C for long-term use. For qPCR, the manufacturer's instructions of Bestar SYBR Green qPCR Master mix kit (DBI Bioscience) were followed. The 20-μl reaction solution was prepared with the following components: 10 μl Bestar SYBR Green qPCR Master mix, 0.5 μl PCR forward primer (10 μM), 0.5 μl PCR reverse primer (10 μM), 1 μl DNA template and 8 μl ddH2O. qPCR was performed using the following thermocycling conditions: Pre-denaturation at 95˚C for 2 min; 40 cycles at 95˚C for 10 sec, 60˚C for 30 sec and 72˚C for 30 sec; and the melting curve was held at 95˚C for 1 min and 55˚C for 1 min. RT-qPCR was repeated three times and the differences in expression levels were calculated using the $2^{-\Delta\Delta Cq}$ method (18). Primers used were as follows: *AGA* forward, 5'-CACTGCTTCTCAAGCTCTTCAT-3' and reverse, 5'-GTTTGTAGGGTCCGCAGTATTT-3'; *MT1E* forward, 5'-CTTTCTTTGCCCTCATTGCCC-3' and reverse, 5'-TACAGTTGGGGTTTGTGTCCC-3'; *TDO2* forward, 5'-GACACTGGATACCGAAGATGAA-3' and reverse, 5'-CACTGCTGAAGTAGGAGCTATC-3'); and *GAPDH* forward, 5'-CATGAGAAGTATGACAACAGCCT-3' and reverse, 5'-AGTCCTTCCACGATACCAAAGT-3'.

Statistical analysis. Date are presented as the mean ± SEM. Histograms were constructed using GraphPad Prism 8 (GraphPad Software, Inc.). Comparisons between two groups were analysed using an unpaired Student's t-test. Comparisons among multiple groups were analysed using one-way ANOVA followed by Bonferroni's post hoc test. Statistical analysis was performed using SPSS software 17.0 (SPSS, Inc.). Experiments were performed in triplicate. $P<0.05$ was considered to indicate a statistically significant difference.

Results

Proteomic expression profiling of ILP-2-related proteins in MCF-7 cells. iTRAQ-based proteomic analysis was used to evaluate the expression profiles of ILP-2-related proteins during MCF-7 cell proliferation. LC-MS/MS analysis generated 55,180 matched spectra, 20,857 peptides and 19,551 unique peptides (Fig. 1A-C). A total of 4,065 proteins were identified by at least one unique peptide with a confidence coefficient >95%. All proteins were subjected to GO analysis and grouped according to biological process, cellular component and molecular function terms (Fig. 1A). These proteins were mainly involved in the biological processes of 'single-organism process', 'cellular process' and 'metabolic process', while 'cell', 'organelle' and 'cell part' accounted for a large portion of proteins in the cellular component term. Additionally, 'catalytic activity' and 'binding' were the two most dominant categories in the molecular function term (Fig. 1A). KEGG analysis revealed that these proteins were mainly involved in the pathways of 'global and overview maps', 'signal transduction' and 'translation' (Fig. 1B). In the top 20 signalling pathways analysed by KEGG, a large number of proteins were associated with 'pathways in cancer', 'endocytosis', 'spliceosome' and 'RNA transport' (Fig. 1C).

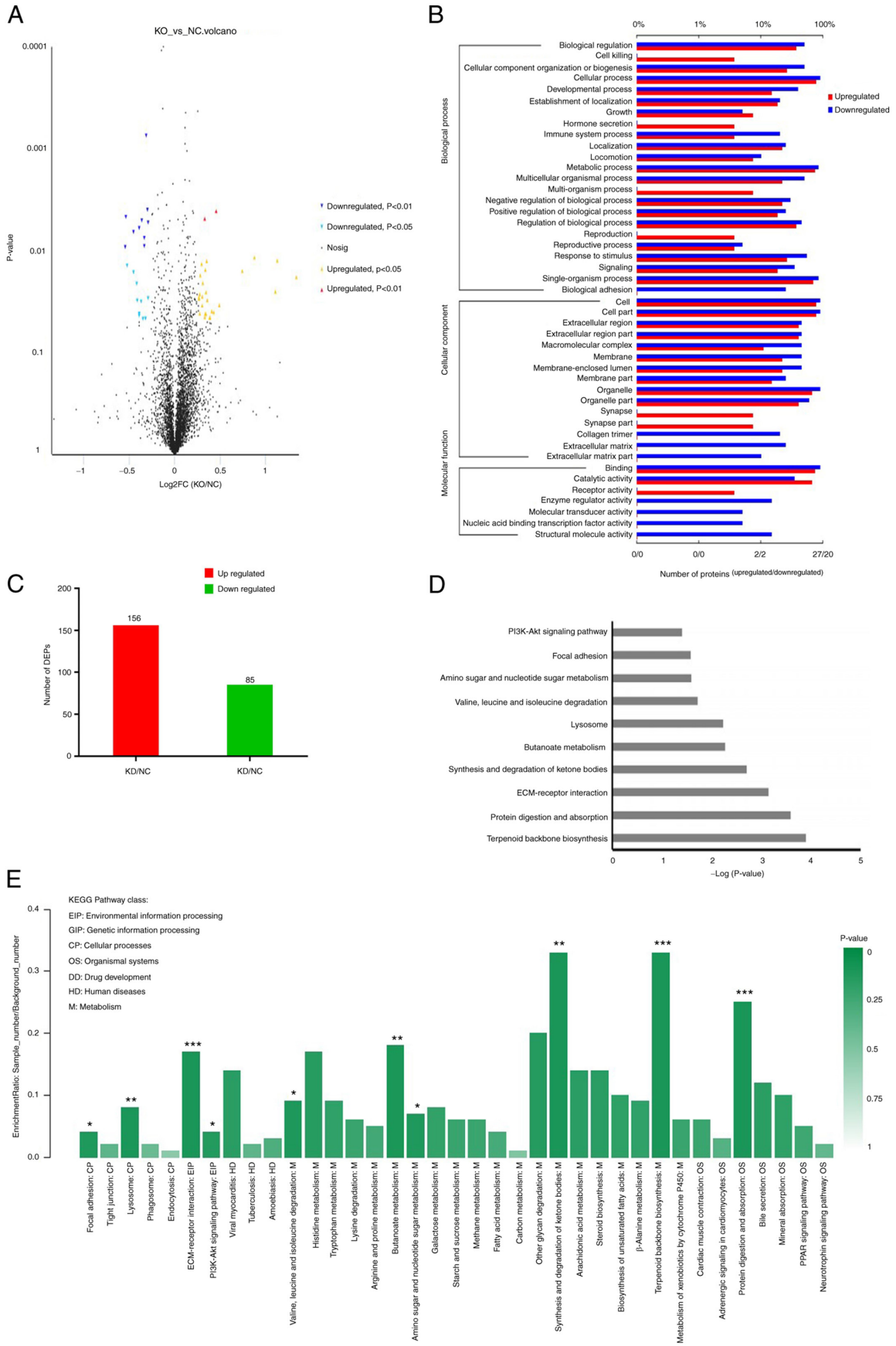

Figure 2. DEPs in the cells of KD (siRNA-5) and NC groups. (A) Volcano plots of DEPs in the KD group vs. NC group. (B) Histogram of upregulated and downregulated protein GO annotation in KD group vs. NC group. The bottom x-axis indicates the number of proteins annotated to a certain GO term. The top x-axis indicates the proportion of proteins annotated to a certain GO term in the total number of proteins with GO term. (C) Number of DEPs in the KD group vs. NC group. (D) The top 10 GO enrichment terms for KEGG pathways (E) Significantly enriched pathways in DEPs, determined by KEGG analysis. *P<0.05, **P<0.01, ***P<0.001 vs. the NC group. DEP, differentially expressed protein; siRNA, small interfering RNA; NC, negative control; KD, knockdown; GO, Gene Ontology; KEGG, Kyoto Encyclopedia of Genes and Genomes.

Table III. Differentially expressed proteins in the KD vs. NC group (fold-change ≥1.66, P<0.05, n=3).

		Protein expression (ng/ml)	
Accession number	Gene symbol	NC	KD
Q9BYX7	*POTEKP*	1.01	2.53
P04732	*MT1E*	1.07	2.33
P20933	*AGA*	1.13	2.42
P48775	*TDO2*	1.01	1.85
A0A0A0MTQ8	*CCDC175*	1.08	1.80

KD, knockdown; NC, negative control; *POTEKP*, putative β-actin-like protein 3; *MT1E*, metallothionein 1E; AGA, N(4)-(β-N-acetylglucosaminyl)-L-asparaginase; TDO2, tryptophan 2,3-dioxygenase; *CCDC175*, coiled-coil domain-containing protein 175.

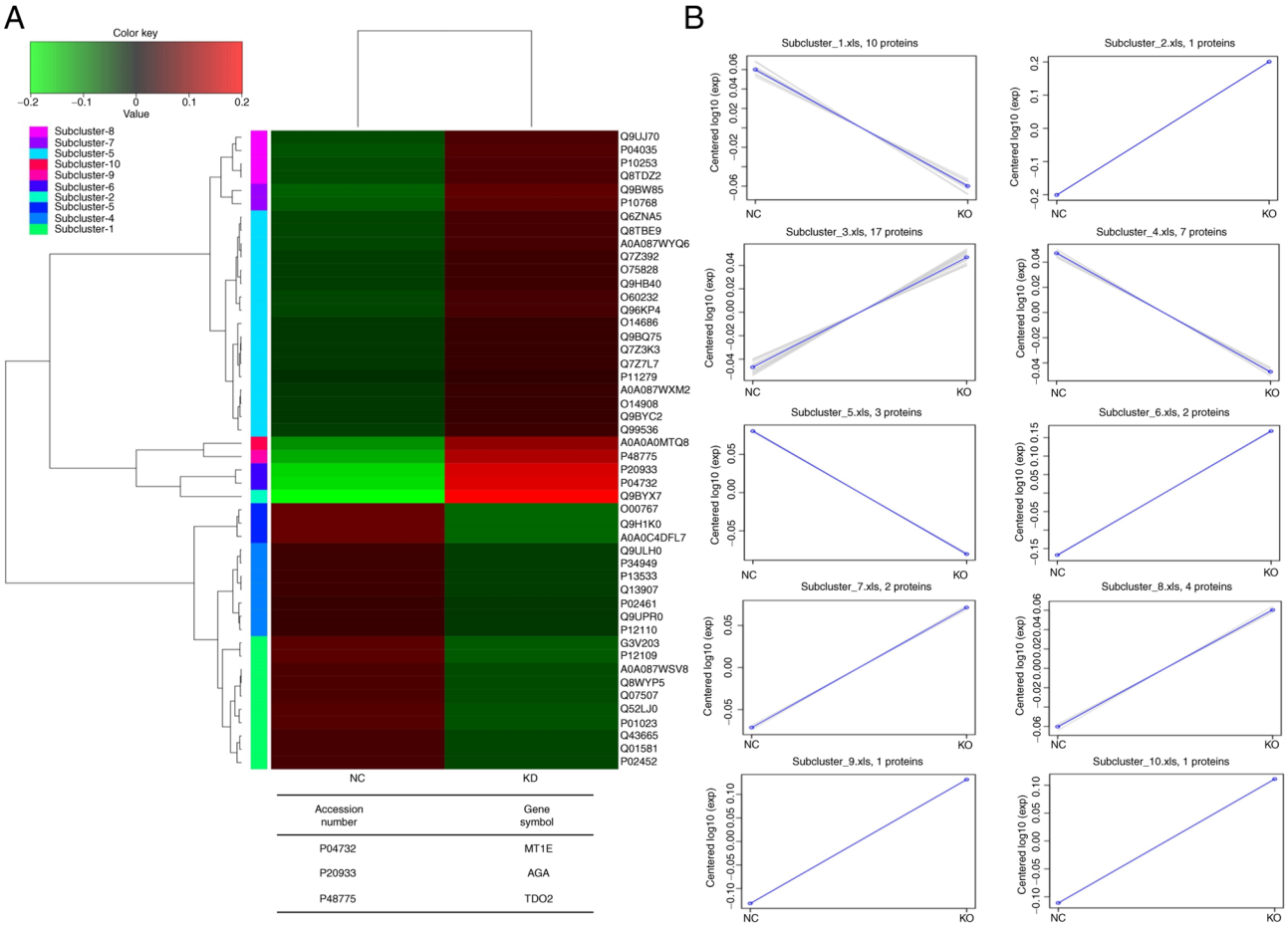

Figure 3. Heatmap and clustering analysis of the expression patterns of DEPs in the KD and NC groups. (A) The heatmap of the DEPs. The table shows the differentially expressed genes in the KD vs. NC group. (B) Sub-clusters 2, 3, 6, 7, 8, 9 and 10 (including 1, 17, 2, 2, 4, 1 and 1 proteins) were upregulated from the NC group to the KD group; sub-clusters 1, 4 and 5 (including 10, 7 and 3 proteins) were downregulated from the NC group to the KD group. DEP, differentially expressed protein; NC, negative control; KD, knockdown; MT1E, metallothionein 1E; AGA, N(4)-(β-N-acetylglucosaminyl)-L-asparaginase; TDO2, tryptophan 2,3-dioxygenase.

Identification of DEPs in ILP-2 KD MCF-7 cells. DEPs were identified between cells transfected with siRNA-5 or NC siRNA clones. ILP-2-related proteins with dynamic changes were analysed during MCF-7 cell proliferation. Therefore, a total of 241 DEPs (FC >1.20 or <0.83; P<0.05) were identified between the siRNA-5 and NC groups (Fig. 2A-C). Among them, 156 proteins were upregulated and 85 were downregulated (Fig. 2B and C). The top 5 DEPs are selectively listed in Table III based on the FC (KD vs. NC) and P-values (FC ≥1.66; P<0.05).

Functional analysis of ILP-2-related proteins in ILP-2 KD MCF-7 cells. To reveal any differences between biological pathways, GO functional enrichment analysis was performed

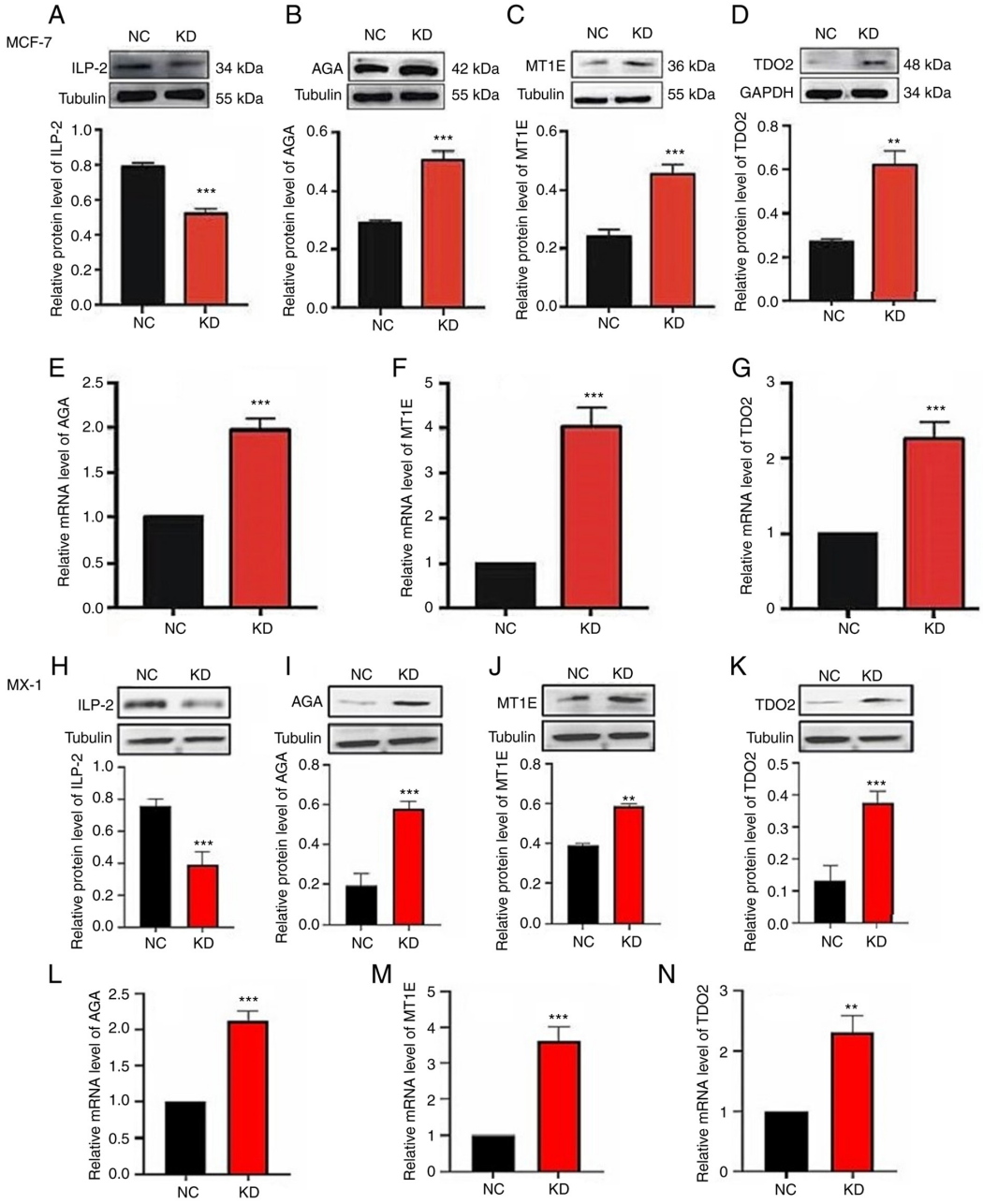

Figure 4. Western blotting and RT-qPCR analyses of the differentially expressed proteins in MCF-7 and MX-1 cells. Knockdown efficiency of KD (siRNA-5) was confirmed via western blotting in (A) MCF-7 and (H) MX-1 cells. Western blotting showed that the relative protein expression levels of (B and I) AGA, (C and J) MT1E and (D and K) TDO2 were increased when ILP-2 expression was knocked down. Tubulin and GAPDH were used as reference proteins. RT-qPCR analysis indicated that the relative mRNA expression levels of (E and L) *AGA*, (F and M) *MT1E* and (G and N) *TDO2* were increased when ILP-2 expression was knocked down. GAPDH was used as the reference gene. Data are presented as the mean ± SEM and groups were compared with an unpaired Student's t-test (n=3). **P<0.01, ***P<0.001 vs. the NC group. RT-qPCR, reverse transcription-quantitative PCR; siRNA, small interfering RNA; ILP-2, inhibitor of apoptosis protein-like protein-2; MT1E, metallothionein 1E; AGA, N(4)-(β-N-acetylglucosaminyl)-L-asparaginase; TDO2, tryptophan 2,3-dioxygenase; NC, negative control.

using the DAVID online tool. Based on GO enrichment analysis, the 241 DEPs were mainly enriched in the terms 'terpenoid backbone biosynthesis', 'protein digestion and absorption', 'ECM-receptor interaction', 'synthesis and degradation of ketone bodies' and 'lysosomes' (Fig. 2D). KEGG pathway analysis revealed that the DEPs were significantly enriched in 'lysosome', 'ECM-receptor interaction', 'butanoate metabolism', 'synthesis and degradation of ketone bodies', 'terpenoid backbone biosynthesis' and 'protein digestion and absorption' (Fig. 2E).

Heatmap of DEPs in ILP-2 KD MCF-7 cells. hcluster was used to perform cluster analysis and illustrate the expression patterns of the aforementioned DEPs (FC ≥1.20 or ≤0.83; P<0.05). Heatmap of DEPs revealed similar expression patterns to KD and NC groups (Fig. 3A). Based on their expression patterns, DEPs were grouped into 10 clusters (Fig. 3B). Some clusters exhibited an overall upregulation pattern between the NC and KD groups, including the sub-clusters 2, 3, 6, 7, 8, 9 and 10 (proteins, 1, 17, 2, 2, 4, 1 and 1, respectively). However, proteins in the remaining clusters exhibited a downregulation

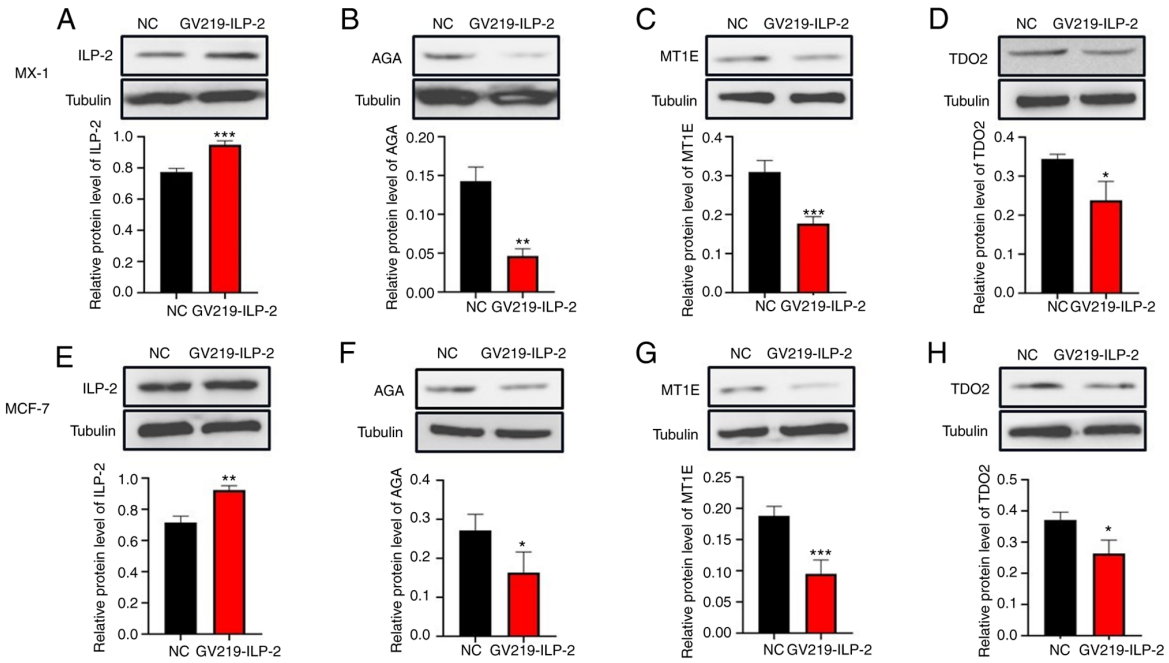

Figure 5. Western blot analysis showed that the relative protein expression levels of AGA, MT1E and TDO2 were decreased when the protein expression of ILP-2 was overexpressed. Tubulin was used as the reference protein. Western blot analysis of (A and E) ILP-2, (B and F) AGA, (C and G) MT1E and (D and H) TDO2 in (A-D) MX-1 and (E-H) MCF-7 cells were decreased when ILP-2 was overexpressed. Tubulin was used as a reference protein. Data are presented as the mean ± SEM and groups were compared with an unpaired Student's t-test (n=3). *P<0.05, **P<0.01, ***P<0.001 vs. the NC group. ILP-2, inhibitor of apoptosis protein-like protein-2; MT1E, metallothionein 1E; AGA, N(4)-(β-N-acetylglucosaminyl)-L-asparaginase; TDO2, tryptophan 2,3-dioxygenase; NC, negative control.

expression pattern between the NC and KD groups (sub-clusters, 1, 4 and 5; proteins, 10, 7 and 3, respectively). The analysed gene numbers were entered into NCBI for matching to find the protein corresponding to the gene (Table III). The final screen identified proteins associated with tumour physiological activity, including AGA, MT1E and TDO2 (Fig. 3A).

Western blotting and RT-qPCR analyses of DEPs. Western blotting and RT-qPCR were performed to validate the iTRAQ results on the mRNA and protein expression levels of AGA, MT1E and TDO2 in ILP-2 KD MX-1 and MCF-7 cells. ILP-2 KD was confirmed in both cell lines (Fig. 4A and H). The results showed that the protein (Fig. 4A-D and H-K) and mRNA (Fig. 4E-G and L-N) expression levels of AGA, MT1E and TDO2 were significantly increased in MX-1 and MCF-7 cells transfected with siRNA targeting ILP-2 compared with in the NC group. ILP-2 overexpression was confirmed in both cell lines (Fig. 5A and E). By contrast, western blotting of ILP-2 overexpression showed that the protein expression levels of AGA, MT1E and TDO2 in MX-1 and MCF-7 cells were significantly reduced compared with in the NC group (Fig. 5B-D and F-H). These results were consistent with those obtained using the iTRAQ technology, both suggesting that the expression levels of AGA, MT1E and TDO2 were associated with the promotive effect of ILP-2 on MCF-7 and MX-1 cell proliferation.

Discussion

Breast cancer is a multifactorial, multistep and heterogeneous disease caused by the uncontrolled proliferation of breast epithelial cells in response to multiple oncogenic factors, such as alcohol consumption, obesity and ageing (19). Although several high-risk factors associated with the development of breast cancer have been reported, the aetiology of the disease has not yet been fully elucidated. The risk of developing breast cancer increases with the accumulation of high-grade risk factors. Several biological processes actively contribute to the development and growth of breast cancer, including protein signalling and other complex cellular biological processes (20-23).

In the present study, a total of 4,065 proteins were identified in MCF-7 breast cancer cells using iTRAQ-based proteomic analysis. The identified proteins were involved in several biological processes, such as cellular process and metabolic process, as well as immune system process. The iTRAQ-based proteomic analysis also revealed that the ILP-2-mediated breast cancer growth. A previous study demonstrated that the expression of ILP-2 is increased in the serum of patients with breast cancer (24). Additionally, immunohistochemical and western blotting assays have shown that ILP-2 is upregulated in breast cancer tissues, and in the breast cancer cell lines MX-1, MCF-7 and HCC-1937 (25,26). These findings indicated that the upregulated expression of ILP-2 in breast cells could be a significant high-risk factor for the development of breast cancer. Nevertheless, the occurrence of breast cancer is not induced by a single risk factor, but is often the result of the synergistic effect of multiple high-risk factors.

To further investigate the effect of ILP-2-related proteins on breast cancer development and progression in the current study, ILP-2 was silenced in MCF-7 cells via cell transfection with corresponding siRNA sequences. Subsequently, the changes in the expression levels of ILP-2-related proteins were

determined. The results showed that 241 proteins were differentially expressed between the ILP-2 KD and control groups. DEPs were significantly enriched in pathways associated with 'lysosome', 'ECM-receptor interaction' and 'butanoate metabolism'. Furthermore, the results revealed that AGA, MT1E and TDO2 were markedly associated with ILP-2. It has been reported that breast cancer progression is associated with cell proliferation, signal transduction and regulation of the immune system (27,28).

In our previous study, silencing assays showed that ILP-2 KD attenuated the proliferation and promoted the apoptosis of MCF-7 and MX-1 breast cancer cells, thus highlighting the effect of ILP-2 on regulating the survival of breast cancer cells. Furthermore, this previous study found the siRNA-5 had a higher KD efficiency on ILP-2 than siRNA-3; therefore, siRNA-5 was applied to knock down ILP-2 in the present study. In addition, ILP-2 silencing inhibited breast cancer cell migration, thus indicating that ILP-2 was not only involved in maintaining breast cancer cell survival, but could also enhance the migratory ability of breast cancer cells (7). The aforementioned findings suggested that the increased expression of ILP-2 in breast cancer cells could enhance the ability of cells to escape apoptosis, and promote cell proliferation and invasion through different biological processes.

To further identify the high-risk factors that promote breast cancer progression synergistically with ILP-2, ILP-2 was knocked down in MCF-7 and MX-1 cells via cell transfection with the corresponding siRNA sequences. Both western blotting and RT-qPCR analysis supported that MT1E, TDO2 and AGA could serve a significant role in breast cancer progression. Previous studies have demonstrated that MT1E upregulation predicted poor prognosis in patients with breast cancer (29,30). Furthermore, TDO2 has been found to promote breast cancer cell migration (31,32), while mutations in the *AGA* gene have been reported to induce the occurrence of lysosomal storage diseases, such as aspartylglucosaminuria (33,34). In the present study, the results of the proteomic analysis revealed that ILP-2 knockdown in breast cancer cells. Additionally, AGA, MT1E and TDO2 were notably upregulated in ILP-2-KD breast cancer cells. Therefore, it was hypothesized that ILP-2 upregulation-mediated breast carcinogenesis could result from the synergistic effect of various high-risk factors, including AGA, MT1E and TDO2. Overall, elevated ILP-2 may cooperate with other proteins, such as AGA, MT1E and TDO2, to inhibit apoptosis and promote the proliferation and invasion of breast cancer cells. However, the current results only indicated that the ILP-2 protein is closely associated with the AGA, MT1E and TDO2 proteins; however, direct evidence of a definite protein-protein interaction between them was not identified, which is something to investigate further in the future.

The aforementioned findings were verified in MCF-7 and MX-1 breast cancer cells following ILP-2 overexpression. The results showed that the expression levels of AGA, MT1E and TDO2 were significantly decreased in ILP-2-overexpressing breast cancer cells. Therefore, the co-expression pattern of AGA, MT1E and TDO2 with ILP-2 could provide novel insights into the association between ILP-2 expression and breast cancer cell proliferation. Additionally, the results suggested that the aforementioned ILP-2 could be involved in the proliferation and growth of breast cancer cells, signal transduction and immune system regulation. It was therefore indicated that ILP-2 may exert a significant effect on regulating the development of breast cancer, while its dysregulated expression in cells could be a key event, eventually leading to breast cancer.

In summary, the current study suggested that ILP-2 could play a significant role in breast cancer cell proliferation and its function could be closely associated with the expression of AGA, MT1E and TDO2, three potential key factors in various regulatory pathways. However, more studies are needed to further explore the mechanism underlying the effect of ILP-2 on breast cancer with emphasis on the prominent proteins implicated. We are also currently intervening in ILP-2 expression by designing ILP-2-targeting drugs and also testing the associated prognosis; these will also be one of the focuses of our future work.

Acknowledgements

The authors would like to thank Dr Benson O.A. Botchway and Akhileshwar Namani, (both from Zhejiang University School of Medicine), Dr Hanmeng (Ningbo University), Dr Mridul Roy (Jishou University School of Medicine) and Dr Wei Zhou (Hunan Agricultural University) for critically revising the manuscript. Furthermore, the authors would like to thank Dr Dan Dan He (Shanghai Majorbio Bio-Pharm Technology Co., Ltd.) for their instruction regarding the experimental study.

Funding

This study was supported by the National Natural Science Foundation of China (grant no. 81360397), Hunan Provincial Natural Science Foundation of China (grant no. 2020JJ4513) and Scientific Research Foundation of Hunan Provincial Education Department of China (grant no. 19A400).

Availability of data and materials

The datasets generated and/or analyzed during the current study are available in the iProX repository, https://www.iprox.cn/page/PSV023.html;?url=1637641893490Nyefandhttps://www.iprox.cn/page/PSV023.html;?url=1640500832317IEB0 (password, deZn).

Authors' contributions

SX and ZZ confirm the authenticity of all the raw data. SX cultured cell lines, performed proteomic sample preparation, interpreted data and drafted the manuscript. LZ contributed to drafting the revised manuscript and interpreted data. ZZ performed the bioinformatics analysis and drafted the manuscript. SW performed western blotting. RC participated in experimental design and critically revised the manuscript. MX designed the study, and drafted and critically revised the manuscript. All authors have read and approved the final manuscript.

Ethics approval and consent to participate

Not applicable.

Patient consent for publication

Not applicable.

Competing interests

The authors declare that they have no competing interests.

References

1. Kimball CC, Nichols CI and Vose JG: The payer and patient cost burden of open breast conserving procedures following percutaneous breast biopsy. Breast Cancer (Auckl) 12: 1178223418777766, 2018.
2. Sung H, Ferlay J, Siegel RL, Laversanne M, Soerjomataram I, Jemal A and Bray F: Global cancer statistics 2020: GLOBOCAN estimates of incidence and mortality worldwide for 36 cancers in 185 countries. CA Cancer J Clin 71: 209-249, 2021.
3. Al-Darwish AA, Al-Naim AF, Al-Mulhim KS, Al-Otaibi NK, Morsi MS and Aleem AM: Knowledge about cervical cancer early warning signs and symptoms, risk factors and vaccination among students at a medical school in Al-Ahsa, Kingdom of Saudi Arabia. Asian Pac J Cancer Prev 15: 2529-2532, 2014.
4. Thomas KH and Ramirez RA: Leptomeningeal disease and the evolving role of molecular targeted therapy and immunotherapy. Ochsner J 17: 362-378, 2017.
5. Costa RLB, Han HS and Gradishar WJ: Targeting the PI3K/AKT/mTOR pathway in triple-negative breast cancer: A review. Breast Cancer Res Treat 169: 397-406, 2018.
6. Qing L and Qing W: Development of epidermal growth factor receptor targeted therapy in pancreatic cancer. Minerva Chir 73: 488-496, 2018.
7. Zhu L, Zhou W, Zhu X, Xiang S, Wang S, Peng Y, Lu B, Tang P, Chen Q, Wu M, *et al*: Inhibitor of apoptosis protein-like protein-2: A novel growth accelerator for breast cancer cells. Oncol Rep 40: 2047-2055, 2018.
8. Xiang M, Zhou W, Gao D, Fang X and Liu Q: Inhibitor of apoptosis protein-like protein-2 as a novel serological biomarker for breast cancer. Int J Mol Sci 13: 16737-16750, 2012.
9. Ouyang H, Wang Z, Chen X, Yu J, Li Z and Nie Q: Proteomic analysis of chicken skeletal muscle during embryonic development. Front Physiol 8: 281, 2017.
10. Campos JM, Neves LX, de Paiva NC, de Oliveira E Castro RA, Casé AH, Carneiro CM, Andrade MH and Castro-Borges W: Understanding global changes of the liver proteome during murine schistosomiasis using a label-free shotgun approach. J Proteomics 151: 193-203, 2017.
11. Liu J, Liu Z, Chen L and Zhang H: iTRAQ-based proteomic analysis reveals alterations in the liver induced by restricted meal frequency in a pig model. Nutrition 32: 871-876, 2016.
12. Minjarez B, Calderón-González KG, Rustarazo ML, Herrera-Aguirre ME, Labra-Barrios ML, Rincon-Limas DE, Del Pino MM, Mena R and Luna-Arias JP: Identification of proteins that are differentially expressed in brains with Alzheimer's disease using iTRAQ labeling and tandem mass spectrometry. J Proteomics 139: 103-121, 2016.
13. Liu YC, Ma WH, Ge YL, Xue ML, Zhang Z, Zhang JY, Hou L and Mu RH: RNAi-mediated gene silencing of vascular endothelial growth factor C suppresses growth and induces apoptosis in mouse breast cancer in vitro and in vivo. Oncol Lett 12: 3896-3904, 2016.
14. Yan F, Wang X, Zhu M and Hu X: RNAi-mediated downregulation of cyclin Y to attenuate human breast cancer cell growth. Oncol Rep 36: 2793-2799, 2016.
15. Wang X, Li Y, Xu G, Liu M, Xue L, Liu L, Hu S, Zhang Y, Nie Y, Liang S, *et al*: Mechanism study of peptide GMBP1 and its receptor GRP78 in modulating gastric cancer MDR by iTRAQ-based proteomic analysis. BMC Cancer 15: 358, 2015.
16. Lu ZM, Zhu Q, Li HX, Geng Y, Shi JS and Xu ZH: Vanillin promotes the germination of antrodia camphorata arthroconidia through PKA and MAPK signaling pathways. Front Microbiol 8: 2048, 2017.
17. Szklarczyk D, Franceschini A, Wyder S, Forslund K, Heller D, Huerta-Cepas J, Simonovic M, Roth A, Santos A, Tsafou KP, *et al*: STRING v10: Protein-protein interaction networks, integrated over the tree of life. Nucleic Acids Res 43 (Database Issue): D447-D452, 2015.
18. Livak KJ and Schmittgen TD: Analysis of relative gene expression data using real-time quantitative PCR and the 2(-Delta Delta C(T)) method. Methods 25: 402-408, 2001.
19. Ju J, Zhu AJ and Yuan P: Progress in targeted therapy for breast cancer. Chronic Dis Transl Med 4: 164-175, 2018.
20. Jitariu AA, Raica M, Cîmpean AM and Suciu SC: The role of PDGF-B/PDGFR-BETA axis in the normal development and carcinogenesis of the breast. Crit Rev Oncol Hematol 131: 46-52, 2018.
21. Zoi I, Karamouzis MV, Adamopoulos C and Papavassiliou AG: RANKL signaling and ErbB receptors in breast carcinogenesis. Trends Mol Med 22: 839-850, 2016.
22. Jana S, Sengupta S, Biswas S, Chatterjee A, Roy H and Bhattacharyya A: miR-216b suppresses breast cancer growth and metastasis by targeting SDCBP. Biochem Biophys Res Commun 482: 126-133, 2017.
23. Wang Y, Zhou J, Wang Z, Wang P and Li S: Upregulation of SOX2 activated LncRNA PVT1 expression promotes breast cancer cell growth and invasion. Biochem Biophys Res Commun 493: 429-436, 2017.
24. Stricker TP, Brown CD, Bandlamudi C, McNerney M, Kittler R, Montoya V, Peterson A, Grossman R and White KP: Robust stratification of breast cancer subtypes using differential patterns of transcript isoform expression. PLoS Genet 13: e1006589, 2017.
25. Shi Y, Yang F, Sun Z, Zhang W, Gu J and Guan X: Differential microRNA expression is associated with androgen receptor expression in breast cancer. Mol Med Rep 15: 29-36, 2017.
26. Finn RS, Dering J, Conklin D, Kalous O, Cohen DJ, Desai AJ, Ginther C, Atefi M, Chen I, Fowst C, *et al*: PD 0332991, a selective cyclin D kinase 4/6 inhibitor, preferentially inhibits proliferation of luminal estrogen receptor-positive human breast cancer cell lines in vitro. Breast Cancer Res 11: R77, 2009.
27. Stavik B, Skretting G, Olstad OK, Sletten M, Dehli Vigeland M, Sandset PM and Iversen N: TFPI alpha and beta regulate mRNAs and microRNAs involved in cancer biology and in the immune system in breast cancer cells. PLoS One 7; e47184, 2012.
28. Vences-Catalán F, Duault C, Kuo CC, Rajapaksa R, Levy R and Levy S: CD81 as a tumor target. Biochem Soc Trans 45: 531-535, 2017.
29. Gurel V, Sens DA, Somji S, Garrett SH, Weiland T and Sens MA: Post-transcriptional regulation of metallothionein isoform 1 and 2 expression in the human breast and the MCF-10A cell line. Toxicol Sci 85: 906-915, 2005.
30. Tai SK, Tan OJ, Chow VT, Jin R, Jones JL, Tan PH, Jayasurya A and Bay BH: Differential expression of metallothionein 1 and 2 isoforms in breast cancer lines with different invasive potential: Identification of a novel nonsilent metallothionein-1H mutant variant. Am J Pathol 163: 2009-2019, 2003.
31. Novikov O, Wang Z, Stanford EA, Parks AJ, Ramirez-Cardenas A, Landesman E, Laklouk I, Sarita-Reyes C, Gusenleitner D, Li A, *et al*: An Aryl hydrocarbon receptor-mediated amplification loop that enforces cell migration in ER-/PR-/Her2-human breast cancer cells. Mol Pharmacol 90; 674-688, 2016.
32. D'Amato NC, Rogers TJ, Gordon MA, Greene LI, Cochrane DR, Spoelstra NS, Nemkov TG, D'Alessandro A, Hansen KC and Richer JK: A TDO2-AhR signaling axis facilitates anoikis resistance and metastasis in triple-negative breast cancer. Cancer Res 75: 4651-4664, 2015.
33. Saarela J, von Schantz C, Peltonen L and Jalanko A: A novel aspartylglucosaminuria mutation affects translocation of aspartylglucosaminidase. Hum Mutat 24: 350-351, 2004.
34. Saarela J, Oinonen C, Jalanko A, Rouvinen J and Peltonen L: Autoproteolytic activation of human aspartylglucosaminidase. Biochem J 378: 363-371, 2004.